Microkinetic modelling of heterogeneous catalysis revisited: adsorption energies can triumph over activation barriers

LukaSkubic[ab] DrejcKopač[a] BlažLikozar[ac] MatejHuš[acd]

[a]National Institute of Chemistry, Department of Catalysis and Chemical Reaction Engineering, Hajdrihova 19, SI-1001 Ljubljana, Slovenia

[b]Jožef Stefan Institute, Department for Materials Synthesis, Jamova 39, SI-1000 Ljubljana, Slovenia

[c]University of Nova Gorica, Vipavska cesta 13, SI-1000 Nova Gorica, Slovenia

[d]Association for Technical Culture (ZOTKS), Založka 65, SI-1000 Ljubljana, Slovenia

PII: S0169-4332(22)01671-3

DOI: https://doi.org/10.1016/j.apsusc.2022.154135

Reference: APSUSC 154135

Applied Surface Science,
https://www.sciencedirect.com/science/article/pii/S0169433222016713?via%3Dihub

Received Date: 29 March 2022

Revised Date: 20 June 2022

Accepted Date: 29 June 2022

Microkinetic modelling of heterogeneous catalysis revisited: adsorption energies can triumph over activation barriers

Luka Skubic[1,2], Drejc Kopač[1], Blaž Likozar[1,3]*, Matej Huš[1,3,4]*

[1] National Institute of Chemistry, Department of Catalysis and Chemical Reaction Engineering, Hajdrihova 19, SI-1001 Ljubljana, Slovenia
[2] Jožef Stefan Institute, Department for Materials Synthesis, Jamova 39, SI-1000 Ljubljana, Slovenia
[3] University of Nova Gorica, Vipavska cesta 13, SI-1000 Nova Gorica, Slovenia
[4] Association for Technical Culture (ZOTKS), Založka 65, SI-1000 Ljubljana, Slovenia

E-mail: blaz.likozar@ki.si, matej.hus@ki.si

Abstract

In mechanistic studies of heterogeneous catalysis, emphasis is usually placed on the reaction barriers of individual reaction steps despite a long-standing empirical understanding of the importance of adsorption interactions. We construct a few archetypal reaction mechanisms and show the contribution of the adsorption interactions to the overall reaction rate. We investigated the degree of rate control and the reaction rate as the function of the adsorption interactions. The results show that even when leaving the reaction barriers intact, changes in the adsorption interaction have profound effects on the overall turn-over frequencies. This was also shown on a real-life example of ethane dehydrogenation. We re-confirm that although finding the rate-determining step is important in catalyst optimisation, improving the adsorption is at least equally important.

Keywords: Catalysis, adsorption, kinetic modelling, reaction rate, turn-over frequencies

Submitted on: March 2022

1 Introduction

Catalysis is a cornerstone of the chemical industry as more than 90 % of all processes take advantage of some kind of catalysis. As catalysts allow the reaction to take place at milder conditions, their performance is intimately connected with the economics of the processes. Thus, targeted catalyst design is crucial for optimizing energy-expensive processes, such as the production of ammonia, CO_2/CO reduction, oil refining. Even marginal improvements translate into billion-dollar savings.[1] [2]

In heterogeneous catalysis, the phase of the catalyst and the reactants differ. Most commonly, the solid catalyst is in contact with liquid or gaseous substrates. Among all catalytic processes, heterogeneous catalysis is the most commonly used. [3] Examples include the Haber-Bosch process for synthesizing ammonia, developed in 1900s [4], which enabled the production of fertilizers. To this date, this process feeds the world population. Moreover, CO oxidation and conversion of NO_x is used in automotive industry for cleaning exhaust gases. Steam reforming, the Ostwald process, the synthesis of sulphuric acid and ethylene/propylene oxide [5], the Ziegler-Natta polymerization [6] and hydrodesulphurization of petroleum are among the most notable examples of heterogeneous catalysis.

The prerequisite for targeted catalyst development is a good description of the process on current catalysts. As Friend *et al.* put it, catalysis is a multiscale process, where chemical processes on the molecular scale, reaction kinetics and mass transport on the macroscale interplay. [7] While historically new catalysts were identified by trial-and-error mechanism, modelling approaches such as density-functional-theory supported kinetic Monte Carlo have recently shown great potential in intelligent catalyst design. [1] [2]

There are two approaches towards catalyst design and optimisation. According to the Sabatier principle, the interactions between the catalyst and the substrate should be neither too strong nor too weak. In catalyst screening, computational methods are employed to calculate the adsorption energies for the reactants on the investigated catalysts. [8] When a more mechanistic insight is sought, the entire pathway is calculated and the focus falls on the transition states. It is presumed that lowering the energy of the transition states, which corresponds to the activation barriers, improves the catalyst performance.

While this is undoubtedly true, proven countless times experimentally, theoretically and computationally, this is only half of the story. In this paper, we show conceptually that the catalyst performance depends strongly on the adsorption energies. We investigate eight different pathways, corresponding to different reaction mechanisms. We exploit the abilities of simulations to probe an idealised, physically unattainable scenario, where the adsorption energies can be changed irrespective of the (fixed) activation barriers. We show that these, too, have a profound effect on the catalyst performance.

This firmly disproves a common misconception that the effect of the interaction strength (adsorption energy) is mostly due to its connection to the activation barrier, as described by the Bell-Evans-Polanyi (BEP) relation [9]: namely that the increase in the adsorption interaction of an intermediate always brings about the decrease in the activation barrier for the corresponding elementary reaction step. We show that the increased adsorption *alone* suffices for higher turn-over frequencies (TOF).

2 Methods

2.1 Microkinetic model

We have developed a microkinetic model to evaluate the effect of the parameters of individual elementary reactions on the catalyst performance. The model describes a surface process (heterogeneous catalyst) of adsorbed gaseous adsorbates. The reaction is modelled in an idealised batch reactor with the following assumptions: dynamic competitive adsorption and desorption, independent surface sites without lateral interactions, constant temperature, no mass transfer limitations, ideal mixing. Essentially, we are modelling an idealised batch reactor.

For the proposed reaction network, we write and solve a system of differential equations for molar balances of individual species in the bulk and on the catalyst. Additionally, the balance of active sites (occupied and vacant) on the catalyst is also considered. For an adsorbed species i, we have $\frac{\mathrm{d}c_i}{\mathrm{d}t} = r_i^{ads} - r_i^{des} + \sum r_{i,n}$, where c_i stands for the bulk concentration, and r's are the reaction rates of adsorption, desorption and n^{th} elementary step on the surface. For gaseous species, the balance is simply $\frac{\mathrm{d}c_i}{\mathrm{d}t} = r_i^{ads} - r_i^{des}$ because we assume that no chemical transformations occur in the bulk phase.

Let us take a simple Langmuir–Hinshelwood reaction as a minimum working example, which is one of the model mechanisms we investigated (see Supplementary Information for similar derivations for the other evaluated mechanisms). The elementary steps are, as follows:

$$A(g) + * \underset{k_{-A}}{\overset{k_A}{\rightleftharpoons}} A^* \tag{1}$$

$$B(g) + * \underset{k_{-B}}{\overset{k_B}{\rightleftharpoons}} B^* \tag{2}$$

$$A^* + B^* \underset{k_{-1}}{\overset{k_1}{\rightleftharpoons}} AB^* + * \tag{3}$$

$$AB^* \underset{k_{-AB}}{\overset{k_{AB}}{\rightleftharpoons}} AB(g) + * \tag{4}$$

where X $(X = A, B)$ denotes a gas component, X^* the adsorbed species and * an empty catalyst site. All the reactions are reversible. For this mechanism, we write the following molar balances:

$$\frac{\partial P_A}{\partial \mathrm{t}} = \left(-\mathrm{k}_A \theta_{empty} P_A + \mathrm{k}_{-A} \theta_A\right) \cdot f \tag{5}$$

$$\frac{\partial P_B}{\partial \mathrm{t}} = \left(-\mathrm{k}_B \theta_{empty} P_B + \mathrm{k}_{-B} \theta_B\right) \cdot f \tag{6}$$

$$\frac{\partial P_{AB}}{\partial \mathrm{t}} = \left(-\mathrm{k}_{-AB} \theta_{empty} P_{AB} + \mathrm{k}_{AB} \theta_{AB}\right) \cdot f \tag{7}$$

$$\frac{\partial \theta_A}{\partial \mathrm{t}} = k_A \theta_{empty} P_A - k_{-A} \theta_A - k_1 \theta_A \theta_B + k_{-1} \theta_{AB} \theta_{empty} \tag{8}$$

$$\frac{\partial \theta_B}{\partial \mathrm{t}} = k_B\,\theta_{empty} P_B - k_{-B}\,\theta_B - k_1\,\theta_A\,\theta_B + k_{-1}\,\theta_{AB}\,\theta_{empty} \tag{9}$$

$$\frac{\partial \theta_{AB}}{\partial \mathrm{t}} = k_{-AB}\,\theta_{empty} P_{AB} - k_{AB}\,\theta_{AB} + k_1\,\theta_A\,\theta_B - k_{-1}\,\theta_{AB}\,\theta_{empty} \tag{10}$$

$$\begin{aligned}\frac{\partial \theta_{empty}}{\partial \mathrm{t}} = -k_A\,\theta_{empty} P_A + k_{-A}\,\theta_A - k_B\,\theta_{empty} P_B + k_{-B}\,\theta_B - k_{-AB}\,\theta_{empty} P_{AB} \\ + k_{AB}\,\theta_{AB} + k_1\,\theta_A\,\theta_B - k_{-1}\,\theta_{AB}\,\theta_{empty}\end{aligned} \tag{11}$$

where θ_X stands for the coverage of the catalyst with the adsorbed species *X* (dimensionless), θ_{empty} represents the fraction of vacant active sites, and P_X is the (partial) pressure of the component in bulk. For gas species balances, the factor of available surface sites must be supplied:

$$f = \frac{N * R * T}{V_{cat}} \tag{12}$$

where *N* is the numerical density of the active sites on the catalyst, *R* is the universal gas constant, *T* the reaction temperature and V_{cat} is the volume of the catalyst.

The system of differential equations was solved in Python using the SciPy package. A general ODE solver (lsoda) was used because it switches automatically between stiff and non-stiff methods.

The aforementioned relations are valid in general regardless of the chemistry. Following a common approach, we use the transition state theory to derive the reaction rate constants, *k*, from adsorption energies and activation barriers. [10] Non-activated adsorption is a kinetic event (barrierless), for which the reaction rate is computed as

$$k_{ads} = \frac{A}{\sqrt{2\,\pi M_{gx}\,k_B\,T}} \tag{13}$$

where *A* stands for the surface area of the active site, M_{gx} is the mass of the adsorbate molecules, k_B is the Boltzmann constant and *T* is the temperature. The reverse reaction represents desorption and *does* contain an energetic term:

$$k_{des} = \frac{k_B\,T}{h}\,e^{\frac{E_{ads,X}}{k_B\,T}} \tag{14}$$

where *h* is the Planck constant and $E_{ads,X}$ is the adsorption energy of the gas species (negative in value).

For surface reactions, the reaction rates can be calculated as:

$$k_{for} = \frac{k_B\,T}{h}\,e^{-\frac{E_{for}}{k_B T}} \tag{15}$$

$$k_{rev} = \frac{k_B\,T}{h}\; e^{-\frac{E_{rev}}{k_B T}} \tag{16}$$

where E_{Afor} and E_{Arev} stand for the activation barriers in the forward and reverse direction. They are linked by the reaction energy *on the surface*.

$$E_{Arev} = E_{Afor} - \Delta E^{*}_{reaction} \tag{17}$$

This is in general different from the energy difference between *gaseous* products and reactants because the catalyst stabilizes them differently.

$$\Delta E^{*}_{reaction} = \Delta E^{vacuum}_{reaction} + \sum E_{ads}\,(products) - \sum E_{ads}\,(reactants) \tag{18}$$

$\Delta E^{vacuum}_{reaction}$ is the reaction energy were the reaction carried out in vacuum, $\sum E_{ads}\,(products)$ and $\sum E_{ads}\,(reactants)$ are the cumulative adsorption energies of all the products and reactants, respectively.

We modelled the reactions in a temperature interval of 300–400 K. The numerical density of active sites varied from 10^{-5} mol to 10^{-2} mol and the catalyst volume was 0,0005 L. Please see the SI for more details.

2.2 Decoupling the reaction energy and the activation barriers

In reality, a change in the activation energy is linked to a change of the reaction energy, which is itself a function of the adsorption energy. Empirically, a linear relation often holds, which is known as the Bell-Evans-Polanyi (BEP) equation [11] [12]:

$$E_A = k_1 + k_2 \cdot \Delta E \tag{19}$$

where k_1 and k_2 are empirical coefficients.

This makes it infeasible to study solely the effect of adsorption interaction on the reaction kinetics in experiments. Hence, we prepare a theoretical set-up, which allows for a consistent investigation of varying the adsorption energies without changing the overall energetics of the reaction or activation barriers.
The following equations (equations 20 – 27) present an example of decoupling the reaction energy and the activation barrier on Langmuir - Hinshelwood reaction mechanism (presented in equations 1-4).

$$k_{ads,A} = \frac{A}{\sqrt{2\,\pi M_{gA}\,k_B\,T}} \tag{20}$$

$$k_{des,A} = \frac{k_B\,T}{h}\; e^{\frac{E_{ads,A}}{k_B T}} \tag{21}$$

$$k_{ads,B} = \frac{A}{\sqrt{2\,\pi M_{gB}\,k_B\,T}} \tag{22}$$

$$k_{des,B} = \frac{k_B\,T}{h}\,e^{\frac{E_{ads,B}}{k_B\,T}} \tag{23}$$

$$k_{for} = \frac{k_B\,T}{h}\,e^{-\frac{E_{Afor}}{k_B T}} \tag{24}$$

$$k_{rev} = \frac{k_B\,T}{h}\,e^{-\frac{E_{Arev}}{k_B T}} = \frac{k_B\,T}{h}\,e^{-\frac{E_{Afor} - \Delta E^{*}_{reaction}}{k_B T}} = \tag{25}$$

$$= \frac{k_B\,T}{h}\,e^{-\frac{E_{for} - \Delta E^{vacuum}_{reaction} + \sum E_{ads}(products) - \sum E_{ads}(reactants)}{k_B T}}$$

$$= \frac{k_B\,T}{h}\,e^{-\frac{E_{for} - E_{react.} - E_{ads,AB} + E_{ads,A} + E_{ads,B}}{k_B T}}$$

$$k_{ads,AB} = \frac{A}{\sqrt{2\,\pi M_{gAB}\,k_B\,T}} \tag{26}$$

$$k_{des,AB} = \frac{k_B\,T}{h}\,e^{\frac{E_{ads,AB}}{k_B\,T}} \tag{27}$$

2.3 Degree of rate control

At the macroscopic level, the performance of the catalyst boils down to the reaction order with respect to individual reactants and the apparent activation energy for the synthesis of the desired product. The reaction order, n_x, with respect to a gaseous species describes how the reaction rate changes with the pressure. [13] Note that the macroscopic expression need not use integer reaction orders and can use fractional terms, such as the reaction between H_2 and Br_2. (DOI: 10.1021/ja01604a013)

However, at the atomistic level, several elementary reactions occur. Their interplay is complex and, although often difficult to decompose and analyse, gives rise to the observed macroscopic behaviour. A common simplification is to identify the slowest (rate-determining) elementary step (RDS) in the mechanism. [13] A broader approach is to calculate the degree of rate control (DRC), which quantifies the contribution (positive or negative) of individual reaction steps to the overall rate of the reaction.

DRC was first introduced by Campbell et al. [14] who defined the term as the quantitative measure of how each reaction step affects the overall reaction rate. DRC is a powerful concept for determining the rate limiting step(s) in complex reaction mechanism systems [15]. Stegelmann et al. [16] used the degree of rate control to research how specific transition states and intermediates control the reaction rate. The degree of rate control for an elementary step *i* is defined as:

$$X_{RC,i} = \frac{k_i}{r}\left(\frac{\partial r}{\partial k_i}\right)_{k_{j\neq i},K_i} = \left(\frac{\partial \ln r}{\partial \ln k_i}\right)_{k_{j\neq i},K_i} \tag{28}$$

where k_i denotes the reaction rate constant, and r is the overall reaction rate. During the calculation, the equilibrium constant K_i is fixed for each elementary step i, as well as all other reaction rate constants $k_{j\neq i}$. Positive values of X_{RC} denote the positively controlling steps, accelerating the overall reaction, while the reaction steps with a negative X_{RC} value inhibit the overall reaction. From the definition of DRC it is evident that a different DRC can be defined for each *desired* product. Usually, most reaction steps will have a value of $X_{\mathrm{RC}} = 0$, meaning they do not influence of the overall reaction rate. [13] [17]

When the reaction rates are approximated with the Arrhenius equation, DRC simplifies to:

$$X_{RC,i} = \frac{k_i}{r}\left(\frac{\partial r}{\partial k_i}\right)_{k_{j\neq i},K_i} = \left(\frac{\partial \ln r}{\partial \ln k_i}\right)_{k_{j\neq i},K_i} = \left(\frac{\partial \ln r}{\partial\left(\frac{-G_i^{0,TS}}{RT}\right)}\right)_{k_{j\neq i},K_i} = \left(\frac{\partial \ln r}{\partial\left(\frac{-G_i^{0,TS}}{RT}\right)}\right)_{G_{j\neq i}^{0,TS},G_m^0} \quad (29)$$

where the Gibbs free energy is constant for all other transition states $j \neq$ i and all intermediates m. This is equivalent to holding the rate constants k_j of all other steps $j \neq i$ and all equilibrium constants K_j constant. [18]

Analogously, one can define the degree of thermodynamic rate control (TRC), where the stability of the transition states is held constant. This conceptually similar metric is defined as:

$$X_{TRC,n} = \frac{1}{r}\left(\frac{\partial r}{\partial\left(\frac{-G_n^0}{RT}\right)}\right)_{G^0_{m\neq n},G^0{}_i^{TS}} = \left(\frac{\partial \ln r}{\partial\left(\frac{-G_n^0}{RT}\right)}\right)_{G^0_{m\neq n},G^0{}_i^{TS}} \quad (30)$$

where the standard-state free energy is constant for all other intermediates $m \neq n$ as well as all the reactants, products and transition states i. This is a fundamentally thermodynamic quantity and does not include the effects of the free energy of the transition states, which play a role in kinetic parameters. [18]

As Campbell has pointed out, both DRC and TRC are analogous in their form and origin with the former explicitly accounting for transition state effects and the latter for the effect of a specific intermediate. The values DRC and TRC can be compared and correlate well. Due to similarities between the two concepts, they are usually used in a more general definition, where the species i could be a transition state *or* an intermediate. In our research, we also used this general degree of rate control, which is defined as:

$$DRC_i = X_i = \frac{1}{r}\left(\frac{\partial r}{\partial\left(\frac{-G_i^0}{RT}\right)}\right)_{G^0_{j\neq i}} = \left(\frac{\partial \ln r}{\partial\left(\frac{-G_i^0}{RT}\right)}\right)_{G^0_{j\neq i}} = \left(\frac{-\partial \ln r}{\partial\left(\frac{G_i^0}{RT}\right)}\right)_{G^0_{j\neq i}} \quad (31)$$

where G_i^0 is the (Gibbs) activation barrier of the elementary step i, which roughly corresponds to the activation barrier, i.e. the energy of a transition state relative to the initial state. Per definition, the sum of DRCs for all reaction steps equals unity. [17]

$$\sum_{steps} X_{RC,i} = \sum_{TSs} DRC_i = 1 \tag{32}$$

3 RESULTS AND DISCUSSION

3.1 Reaction scenarios

In our analysis, we constructed eight simplified reaction scenarios, ranging from a simple Langmuir-Hinshelwood reaction to more complex two step reaction mechanisms. The mechanisms are written out in full in Scheme 1, while the corresponding kinetic and thermodynamic parameters (barriers, energies) and differential equations are detailed in SI.

In our investigation, we focus on calculating the differences in turn-over frequencies (TOF) and the general degree of rate control instead of TRC for two reasons. First, DRC and TRC are correlated. Second, while the TRC will be dependent on the adsorption energies of the intermediates *per definition*, the turnover frequencies actually provide the information on catalyst performance.

The parameters were chosen to be comparable across scenario and to correspond to real-world values. This means that adsorption energies for stable species range from –0.3 to –0.5 eV and activation barriers from 0.4–0.9 eV. Reaction steps including species that are not stable in the gaseous phase have very large gaseous reaction energies (3 eV), which are compensated by strong adsorption on the catalyst. In Figure 1, we show the evolution of the gaseous phase (*i.e.*, the partial pressure of reactants and products) and the coverage on the catalyst surface for the investigated scenarios. We prove that the reaction systems reach stationary states in the investigated time period and that the chosen reaction parameters are reasonable.

Scheme 1: The reaction steps considered in each scenario.

$A\,(g) + * \underset{k_{-\mathrm{A}}}{\overset{k_{\mathrm{A}}}{\rightleftharpoons}} A^*$ $B\,(g) + * \underset{k_{-B}}{\overset{k_B}{\rightleftharpoons}} B^*$ $A^* + B^* \underset{k_{-1}}{\overset{k_1}{\rightleftharpoons}} AB^* + *$ $AB^* \underset{k_{-\mathrm{AB}}}{\overset{k_{AB}}{\rightleftharpoons}} AB\,(g) + *$	$A\,(g) + * \underset{k_{-\mathrm{A}}}{\overset{k_{\mathrm{A}}}{\rightleftharpoons}} A^*$ $A^* + B \underset{k_{-1}}{\overset{k_1}{\rightleftharpoons}} AB^*$ $AB^* \underset{k_{-\mathrm{AB}}}{\overset{k_{AB}}{\rightleftharpoons}} AB\,(g) + *$
I. Langmuir – Hinshelwood reaction	II. Eley – Rideal reaction
$A\,(g) + * \underset{k_{-\mathrm{A}}}{\overset{k_{\mathrm{A}}}{\rightleftharpoons}} A^*$ $A^* \underset{k_{-1}}{\overset{k_1}{\rightleftharpoons}} B^*$ $B^* \underset{k_{-B}}{\overset{k_B}{\rightleftharpoons}} B\,(g) + *$	$A\,(g) + * \underset{k_{-\mathrm{A}}}{\overset{k_{\mathrm{A}}}{\rightleftharpoons}} A^*$ $A^* + B \underset{k_{-1}}{\overset{k_1}{\rightleftharpoons}} AB\,(g) + *$

III. Monomolecular reaction	IV. Eley – Rideal reaction with a gaseous product
$A\,(g) + * \underset{k_{-A}}{\overset{k_A}{\rightleftharpoons}} A^*$ $B\,(g) + * \underset{k_{-B}}{\overset{k_B}{\rightleftharpoons}} B^*$ $A^* + B^* \underset{k_{-1}}{\overset{k_1}{\rightleftharpoons}} AB^* + *$ $AB^* \underset{k_{-2}}{\overset{k_2}{\rightleftharpoons}} P^*$ $P^* \underset{k_{-P}}{\overset{k_P}{\rightleftharpoons}} P\,(g) + *$	$A\,(g) + * \underset{k_{-A}}{\overset{k_A}{\rightleftharpoons}} A^*$ $A^* \underset{k_{-1}}{\overset{k_1}{\rightleftharpoons}} I^*$ $B + * \underset{k_{-B}}{\overset{k_B}{\rightleftharpoons}} B^*$ $I^* + B^* \underset{k_{-2}}{\overset{k_2}{\rightleftharpoons}} P^* + *$ $P^* \underset{k_{-P}}{\overset{k_P}{\rightleftharpoons}} P\,(g) + *$
V. Sequential reaction	VI. Two-step reaction
$A\,(g) + * \underset{k_{-A}}{\overset{k_A}{\rightleftharpoons}} A^*$ $B\,(g) + * \underset{k_{-B}}{\overset{k_B}{\rightleftharpoons}} B^*$ $C\,(g) + * \underset{k_{-C}}{\overset{k_C}{\rightleftharpoons}} C^*$ $A^* + B^* \underset{k_{-1}}{\overset{k_1}{\rightleftharpoons}} AB^* + *$ $A^* + C^* \underset{k_{-2}}{\overset{k_2}{\rightleftharpoons}} AC^* + *$ $AB^* \underset{k_{-AB}}{\overset{k_{AB}}{\rightleftharpoons}} AB\,(g) + *$ $AC^* \underset{k_{-AC}}{\overset{k_{AC}}{\rightleftharpoons}} AC\,(g) + *$	$A\,(g) + * \underset{k_{-A}}{\overset{k_A}{\rightleftharpoons}} A^*$ $A^* + * \underset{k_{-1}}{\overset{k_1}{\rightleftharpoons}} B^* + C^*$ $B^* \underset{k_{-B}}{\overset{k_B}{\rightleftharpoons}} B\,(g) + *$ $C^* \underset{k_{-C}}{\overset{k_C}{\rightleftharpoons}} C\,(g) + *$
VII. Competitive reaction	VIII. Dissociation reaction

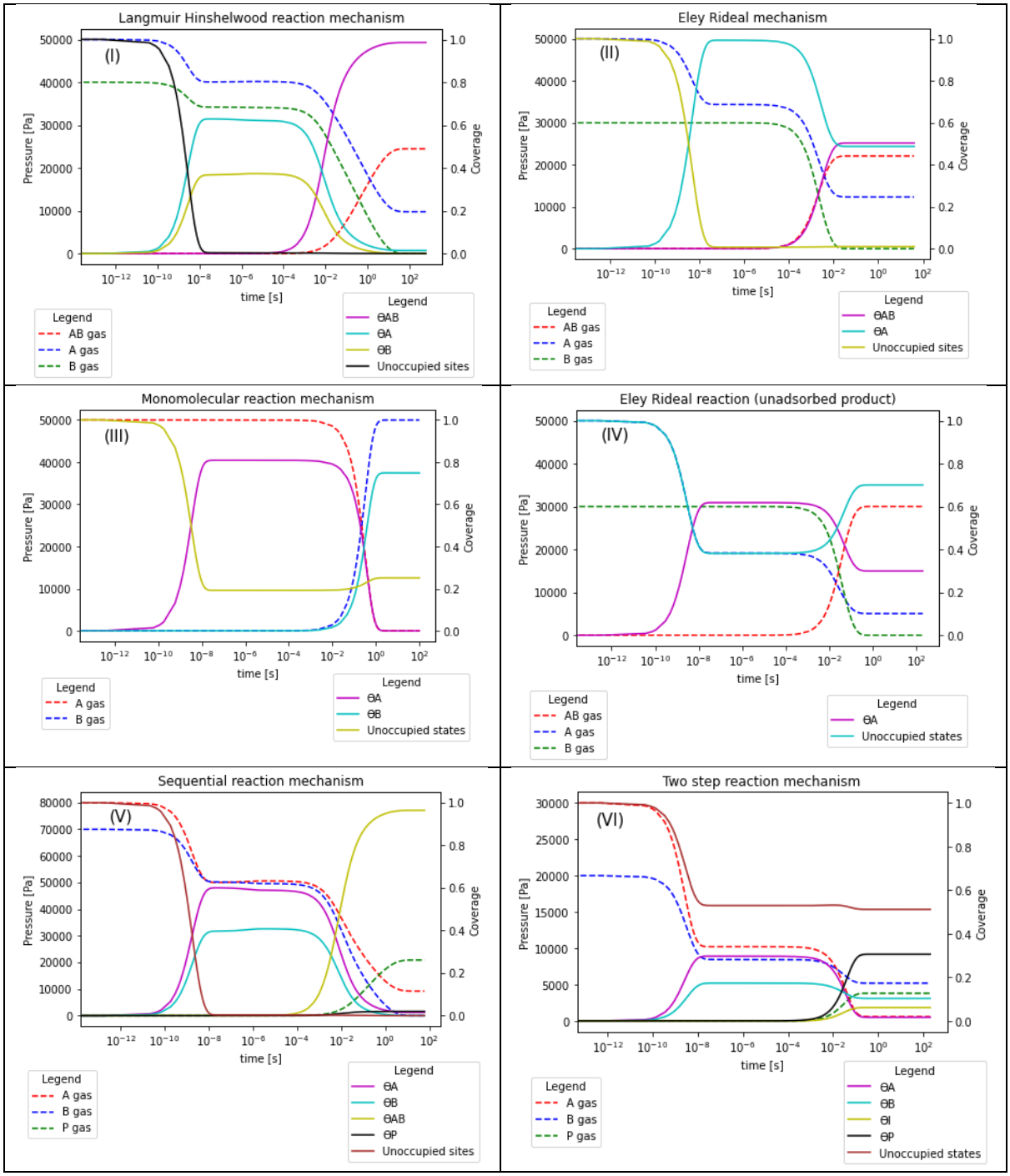
Langmuir Hinshelwood reaction mechanism
(I)
Pressure [Pa]
Coverage
time [s]
Legend
AB gas
A gas
B gas
Legend
ΘAB
ΘA
ΘB
Unoccupied sites
Eley Rideal mechanism
(II)
Pressure [Pa]
Coverage
time [s]
Legend
AB gas
A gas
B gas
Legend
ΘAB
ΘA
Unoccupied sites
Monomolecular reaction mechanism
(III)
Pressure [Pa]
Coverage
time [s]
Legend
A gas
B gas
Legend
ΘA
ΘB
Unoccupied states
Eley Rideal reaction (unadsorbed product)
(IV)
Pressure [Pa]
Coverage
time [s]
Legend
AB gas
A gas
B gas
Legend
ΘA
Unoccupied states
Sequential reaction mechanism
(V)
Pressure [Pa]
Coverage
time [s]
Legend
A gas
B gas
P gas
Legend
ΘA
ΘB
ΘAB
ΘP
Unoccupied sites
Two step reaction mechanism
(VI)
Pressure [Pa]
Coverage
time [s]
Legend
A gas
B gas
P gas
Legend
ΘA
ΘB
ΘI
ΘP
Unoccupied states

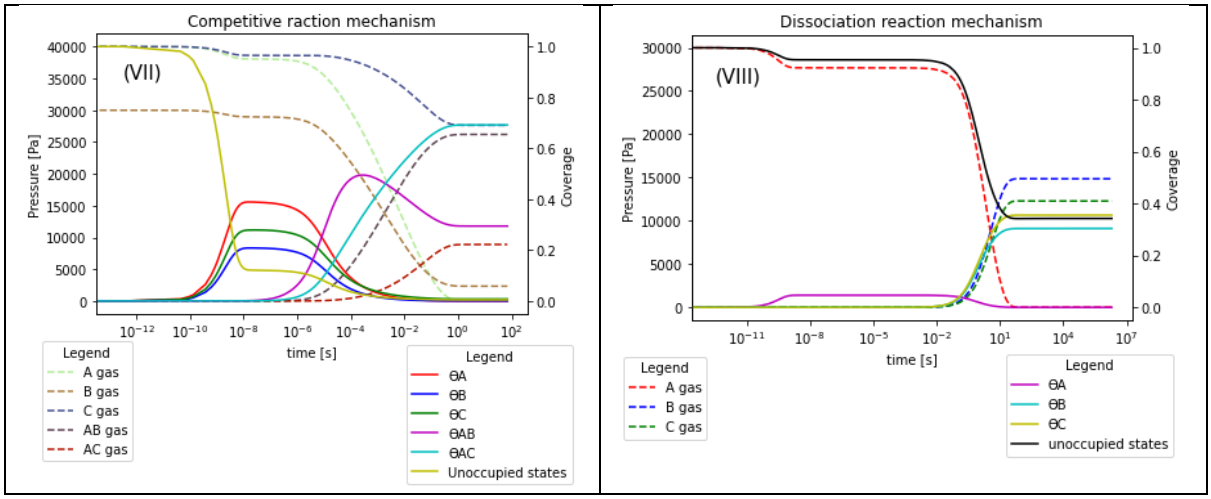

Figure 1: Partial pressures in bulk and coverage of the catalyst surface as a function of time for the scenarios, depicted in Scheme 1. (I) Langmuir - Hinshelwood reaction, (II) Eley – Rideal mechanism, (III) Monomolecular reaction, (IV) Eley – Rideal reaction with unadsorbed product, (V) Sequential reaction, (VI) Two step reaction, (VII) Competitive reaction, (VIII) Dissociation reaction mechanism.

3.2 DRC analysis

3.2.1 Determination of the DRC values

First, we analyse how each reaction step in a given scenario influences the overall reaction rate. The DRC toolbox is a sensitivity analysis, which ascribes a numerical value between –1.0 and +1.0 to each reaction step so that the sum of all DRC values adds up to unity. While the step with the largest DRC value is denoted a rate-determining step (RDS), the term loses its significance when there are several steps with comparable DRC values.

In Table 2, the calculated DRC values for the initial conditions are given. Already from this analysis alone, which does not decompose the reaction rates into different contributions (see Eq. 19–22), it is apparent that the reactant *adsorptions* have non-negligible effects on the overall reaction rate. For a graphical depiction, the reader is referred to the supplementary information.

Scheme 2: Calculated DRC values for different reaction scenarios with an initial set of the kinetic and thermodynamic parameters.

I. Langmuir - Hinshelwood (DRC values are calculated for AB production)

Parameter	DRC value
E_{adsA}	0.31
E_{adsB}	0.52
E_{adsAB}	-0.80
E_{for}	0.97
E_{react}	0.0

II. Eley – Rideal (DRC values are calculated for AB production)

Parameter	DRC value
E_{adsA}	0.21
E_{adsAB}	-0.21
E_{for}	1.0
E_{react}	0.0

Parameter	DRC value
E_{adsA}	0.06
E_{adsB}	0.0

Parameter	DRC value
E_{adsA}	0.19
E_{for}	0.81

E_{for}	0.94
E_{react}	0.0

III. Monomolecular reaction (DRC values are calculated for B production reaction)

Parameter	DRC value
E_{adsA}	-0.02
E_{adsB}	0.14
E_{adsAB}	-0.05
E_{adsP}	-0.08
E_{for1}	0.66
E_{react1}	0.0
E_{for2}	0.30
E_{react2}	0.05

IV. Eley - Rideal reaction with unadsorbed product (DRC values are calculated for product AB, Scheme 1 IV)

E_{react}	0.0

Parameter	DRC value
E_{adsA}	0.45
E_{adsB}	-0.26
E_{adsP}	-0.21
E_{adsI}	-0.60
E_{for2}	0.99
E_{react2}	0.0
E_{for4}	0.03
E_{react4}	0.60

V. Sequential reaction (DRC values are calculated for product P production)

Parameter	DRC value
E_{adsA}	0.41
E_{adsB}	0.67
E_{adsC}	-0.38
E_{adsAB}	-0.65
E_{adsAC}	0.0
E_{for1}	0.97
E_{react1}	0.0
E_{for2}	-0.02
E_{react2}	0.0

VI. Two step reaction mechanism (DRC values are calculated for product P production)

Parameter	DRC value
E_{adsA}	0.55
E_{adsB}	-0.27
E_{adsC}	0.72
E_{adsAB}	-0.01
E_{adsAC}	-0.96
E_{for1}	-0.07
E_{react1}	0.0
E_{for2}	1.04
E_{react2}	0.0

VII. Competitive reaction (DRC values are calculated for AB production reaction)

VIIa. Competitive reaction (DRC values are calculated for AC production reaction)

Parameter	DRC value
E_{adsA}	0.77
E_{adsB}	-0.65
E_{adsC}	0.0
E_{for}	0.88
E_{react}	0.0

VIII. Dissociation reaction mechanism (DRC values are calculated for product B)

For instance, in the Langmuir-Hinshelwood mechanism (Scenario I), the combined DRC for the adsorption of both reactants equals 0.83, which is comparable to the DRC for the surface reaction of the actual chemical transformation (0.97). Analogously, the DRC value for the adsorption of the product is equally *negative*, meaning that a strong interaction of the product

with the catalyst impedes the reaction. In a subsequent section, the effect of the adsorption *energies* will be studied, which is more relevant especially in more complex scenarios, where intermediates (which cannot realistically desorb) participate.

In Scenario II, the reaction rate is primarily governed by the Eley-Rideal step, where a gaseous molecule binds to the adsorbed reactant. The DRC for the adsorption steps of both, one reactant and the product, are noticeably smaller. The same holds true for the monomolecular reaction (Scenario III), where the overall rate depends almost exclusively on the chemical transformation on the surface, and the variation of the Eley-Rideal reaction where the product does not bind to the surface (Scenario IV).

When the surface reaction consists of two sequential steps (Scenario V), the DRC is mostly governed by both conversion steps but not exclusively. The effect of the adsorption energies is smaller but noticeable. The two-step reaction (Scenario VI) is a variation thereof, where the order of the monomolecular and bimolecular steps is reversed. Again, the chemical conversion is the most important reaction but the adsorption energies of the reactants, intermediates and products play an important role (DRCs up to 0.44).

When dealing with the competitive reaction mechanism, there is no unambiguous with respect to *which* product the DRC is defined. It makes intuitive sense to choose the desired product. In our general treatment, we calculate two sets of DRC values; for the product AB and the product AC (Scenarios VII and VIIa). Again, the adsorption of the reactants and intermediates strongly affects the reaction. The DRC value for the adsorption of both required reactants is positive, while it is negative for the reactant leading only to the undesired product.

Lastly, we turn our attention to the dissociation. Unsurprisingly, this reaction, although governed mostly by the chemical decomposition on the catalyst, is strongly influenced by the adsorption interactions. The DRC for the adsorption of the reactant is +0.77, while for the adsorption of the products it is –0.65.

While DRC describes the sensitivity of the overall reaction rate upon the rates of individual steps, we now turn our attention to the dependence of DRC upon the reaction energies. For instance, for exceedingly fast surface reactions or for very strong adsorptions, the DRC value will be insensitive to the change of these values. On the other hand, for slow (RDS) reactions the DRC will be large and also very sensitive to any changes in the underlying energetics as even a small change in the reaction step parameters can cause the given reaction step to cease to be the RDS. As DRCs sum to unity *per* definition, this means the values for other steps will change, as well.

3.2.2 Changing the adsorption interaction

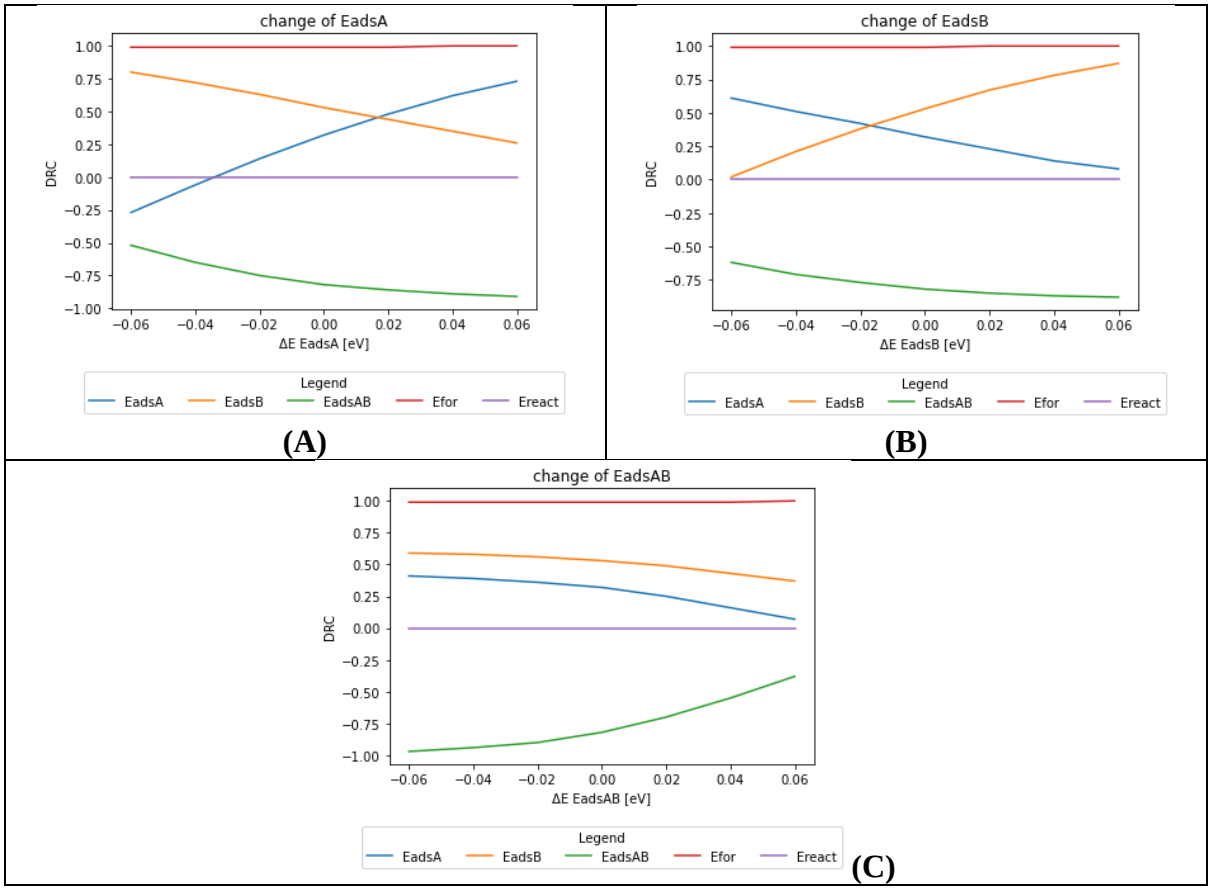

Figure 2: A change in the DRC values when changing the adsorption energies of the adsorbed species in Langmuir – Hinshelwood reaction mechanism, Scenario I.

In Figure 2, the effect of changing the energies on DRC is shown graphically for the Langmuir-Hinshelwood mechanism (Scenario I). We vary the energy of adsorption for the reactants A (Figure 2a) and B (Figure 2b), and the product AB (Figure 2c). While the surface reaction remains the rate determining-step regardless, adversely changing the adsorption energy of either reactant pushes the DRC of the corresponding adsorption step to high values. If the adsorption is too weak, it becomes the RDS. Conversely, a too strong adsorption results in negative DRC. For the product (*AB*), the converse is true and a weaker adsorption facilitates the reaction.

In the simple Eley-Rideal mechanism (Scenario II), the behaviour is analogous to the Langmuir-Hinshelwood mechanism. The DRC values of both adsorption steps (of the reactant and product) are opposite in sign and the same in magnitude. The chemical transformation remains the rate-determining step, while the effect of the adsorptions of the reactant and product is decisive when they are weak or strong, respectively. This is essentially the Sabatier principle.

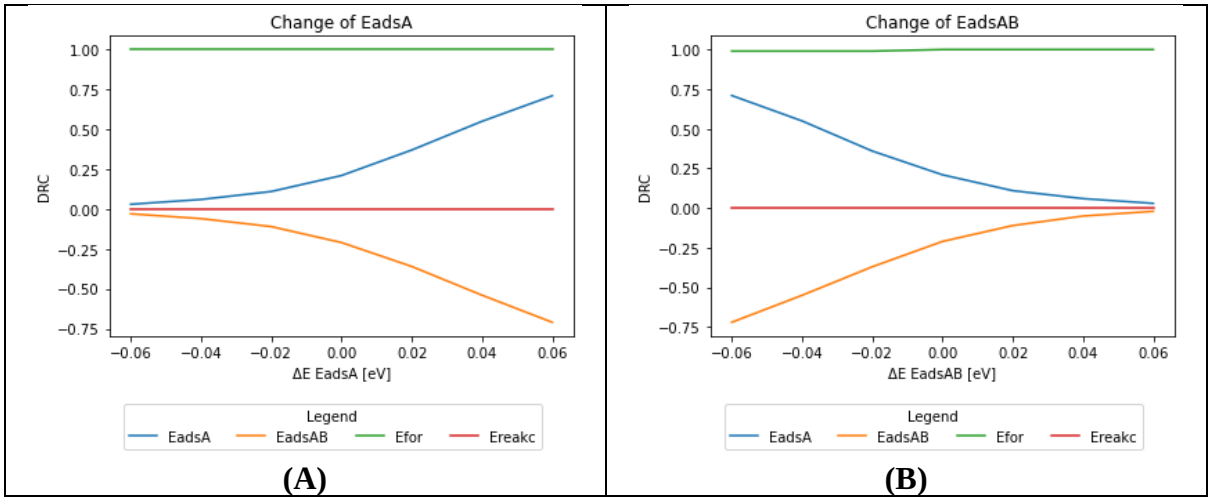

Figure 3: A change in the DRC values when changing the adsorption energies of the adsorbed species in Scenario II.

For the monomolecular reaction mechanism (Scenario III) and the simplified Eley-Rideal mechanism (Scenario IV), only the DRC of the chemical transformation remains non-zero (not shown).

Let us turn to more complicated examples. In the sequential mechanism (Scenario V), A and B must first adsorb, react to form an intermediate (AB), which transforms to the product (P). As shown in Figure 4, a change of any adsorption energy has a (moderate) effect on the DRC values for the transformation reactions and, understandably, a larger effect on the DRC values for the adsorption reactions. In general, the increase (or decrease) of the adsorption interaction for the reactants decreases (or increases) the DRC value of that adsorption reaction and vice-versa for the reaction of the other reactant. When the adsorption interaction of the intermediates or the product changes, the DRC values remain relatively stable and small in magnitude.

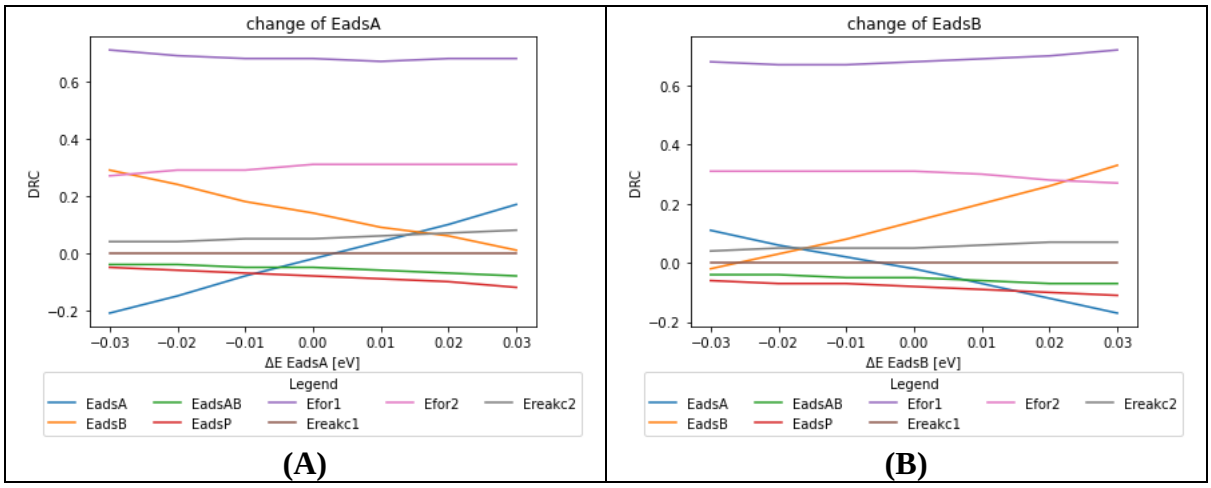

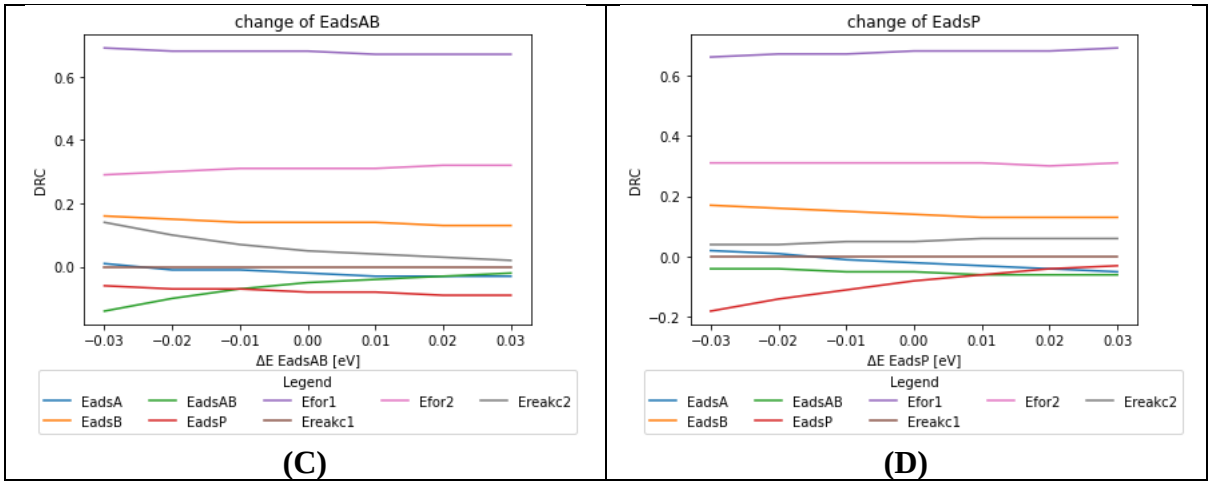

Figure 4: A change in the DRC values when changing the adsorption energies of the adsorbed species in Scenario V.

In the two-step mechanism (Scenario VI), the reactant (A) first converts to the intermediate (I), which then reacts with the second reactant (B) to form the product (B). In Figure 5, the DRC analysis is shown. Decreasing the adsorption interaction of A increases its DRC value, while it depresses the DRC of other adsorption steps. The second reactant B has a negative DRC, which is increased if the adsorption interaction gets weaker. A similar trends is encountered when the interaction of the intermediate and the end product with the catalyst is fine-tuned. Both exhibit negative DRC values, meaning that their adsorption impedes the reaction, and can be increased if this interaction is made weaker. This shows the importance of adsorption energies in specific reaction mechanism.

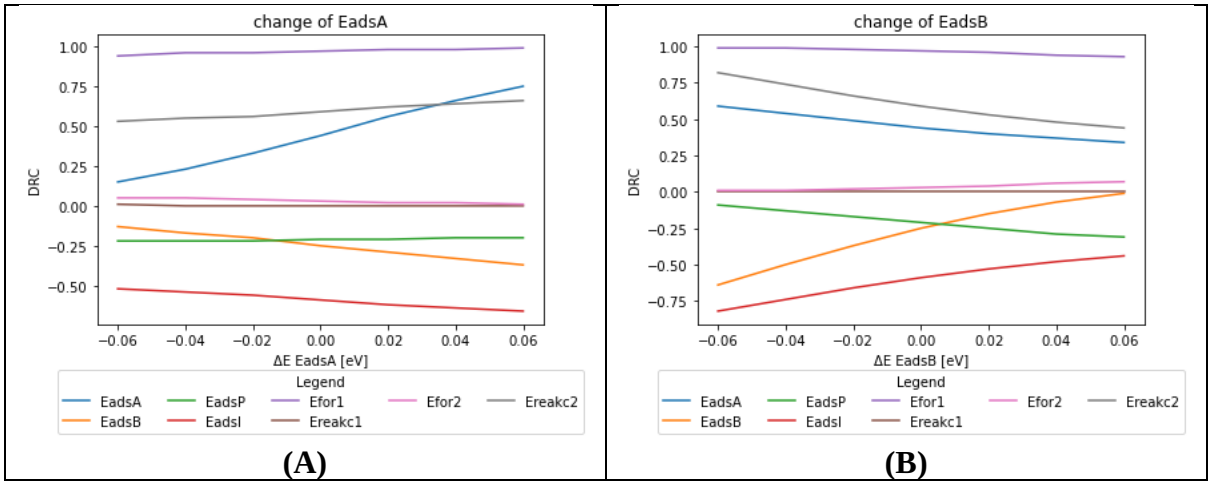

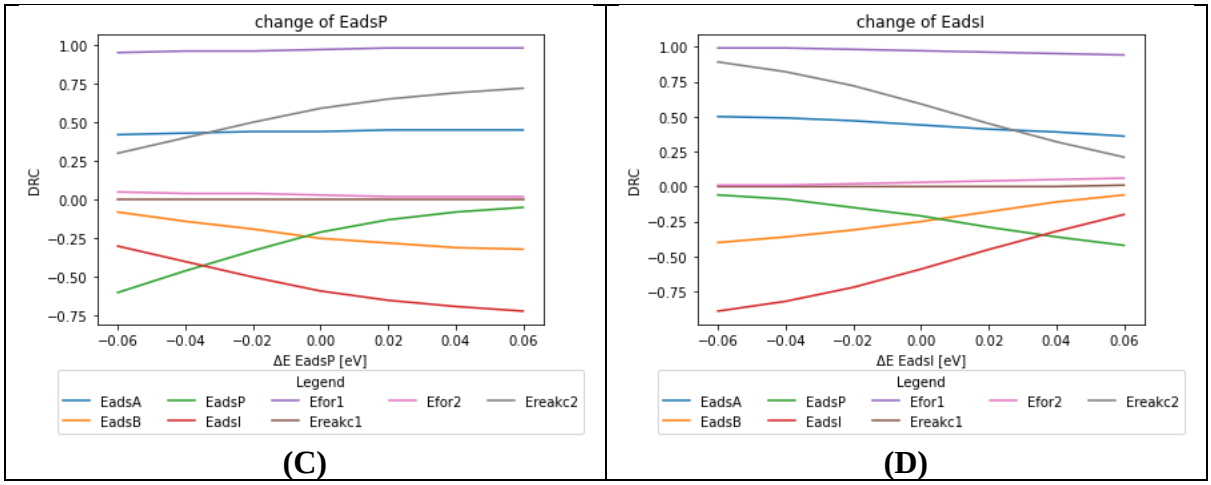

Figure 5: A change in the DRC values when changing the adsorption energies of the adsorbed species in Scenario VI.

In Figure 6, a more complex scenario (Competitive reaction mechanism) is analysed, where A* can react with either B* or C*. Without loss of generality, we deem AB as the desired product and AC as the side product. With respect to the formation of AB, the corresponding chemical transformation is the RDS with the largest DRC, which is, however, not equal to 1.00. In all cases, the adsorption of A and B has a strong positive effect on the reaction rate. Improving their adsorption accelerates the reaction. The opposite is true for the species C. It is also advantageous if the AB does not bind strongly to the catalyst.

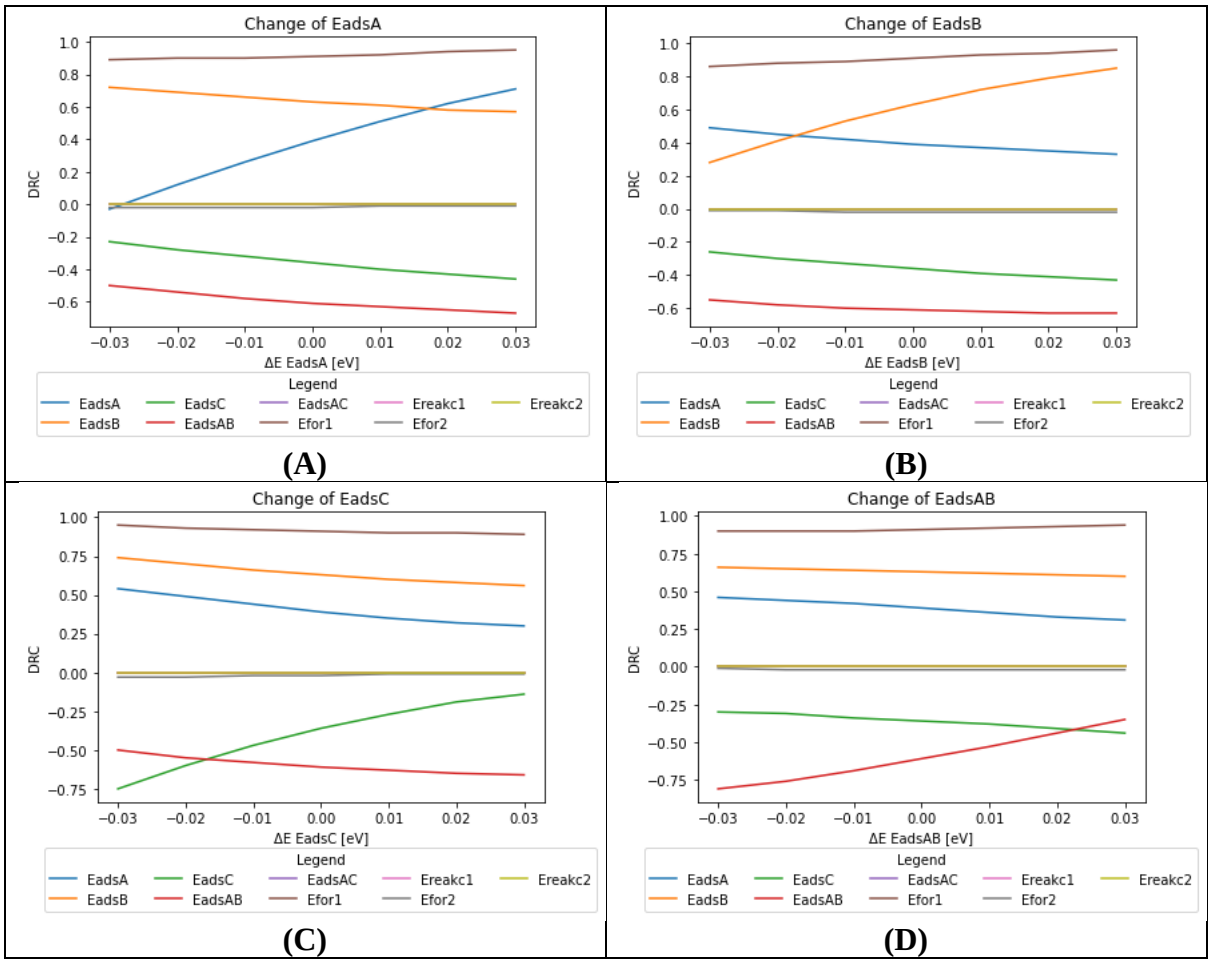

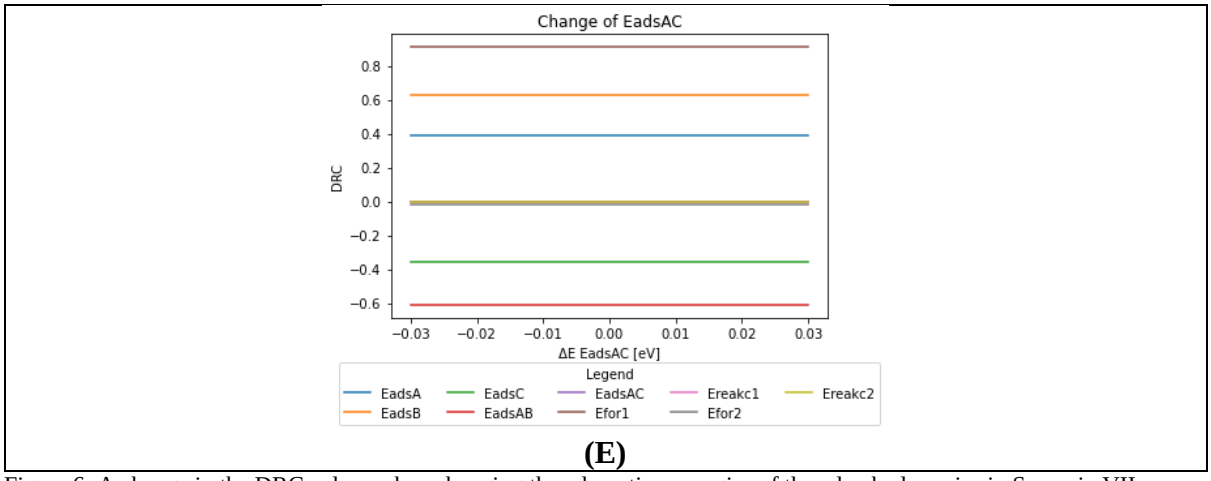

Figure 6: A change in the DRC values when changing the adsorption energies of the adsorbed species in Scenario VII.

An increase in the DRC value *does not* mean that the overall reaction is faster. A large value merely identifies the RDS step. This is obvious when DRC increases if the adsorption of the reactant is impeded because this step becomes the bottleneck of the reaction. However, the DRC analysis tells us if it makes sense to attempt optimising the catalyst for a particular property. In the next section, we focus to the reaction rates.

3.3 Effect on the turnover frequency

In the previous section, we investigated the effect of the adsorption energies on the *sensitivity* of the system. While this is an important piece of information, DRCs only tell us if there is a fundamental change in the reaction control as a consequence of the varying adsorption energies. Yet we are ultimately interested in the effect these change have on the turnover frequencies (TOF), *i.e.* the productivity of the catalyst. Whenever DRC of a reaction is non-zero, this will happen.

In Figure 7, we show the relative reaction rate (with respect to the formation of the product) as a function of changes in the energies.

As a general observation, lowering the activation barrier has the largest effect on the reaction rate, which can be predicted from the Arrhenius relation ($e^{\frac{-E_A}{kT}}$). At 300 K and 400 K, the rate of an individual reaction step is increased 10-fold by a 0.06 eV and 0.08 eV decrease in activation barrier, respectively. Conversely, an increase in the barrier decreases the rate. As these steps generally have large DRCs (approaching unity), this change is mirrored in the overall production rate. In the competitive reaction scenario, only the barrier yielding the desired product has any effect on this production.

Fine-tuning the adsorption interaction irrespective of the reaction barriers further on in the mechanism can also improve the turn-over frequencies. In the Langmuir-Hinshelwood mechanism (Scenario I), decreasing the adsorption strength of the reactant B for 0.06 eV doubles the reaction rate. Conversely, weakening the interaction of the final product (AB) *increases* the turnover frequency. A 0.05 eV decrease in the interaction yields a 3-fold speed-up. In the Eley-Rideal mechanisms (Scenarios II and IV), the dependence is smaller but the trend is the same. The reaction is accelerated if the products desorb more weakly. In the monomolecular transformation (Scenario III), there is very little dependence upon the adsorption interaction.

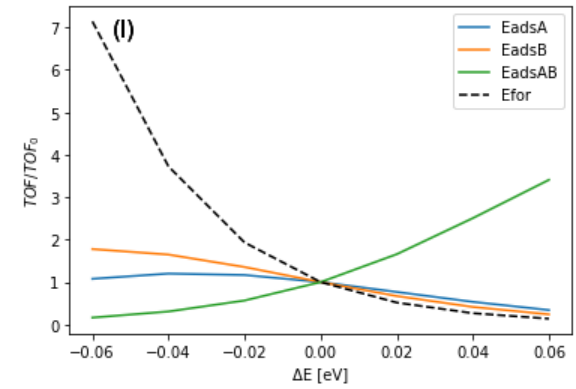

I. Langmuir – Hinshelwood reaction

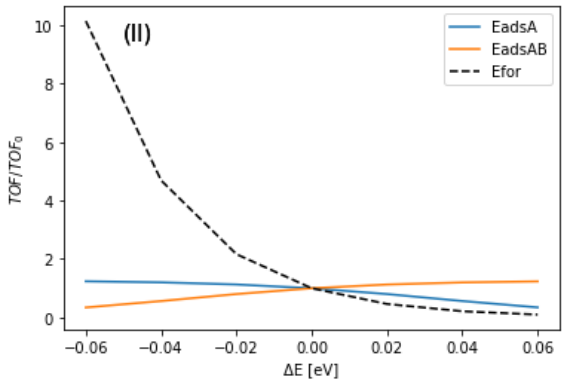

II. Eley – Rideal reaction

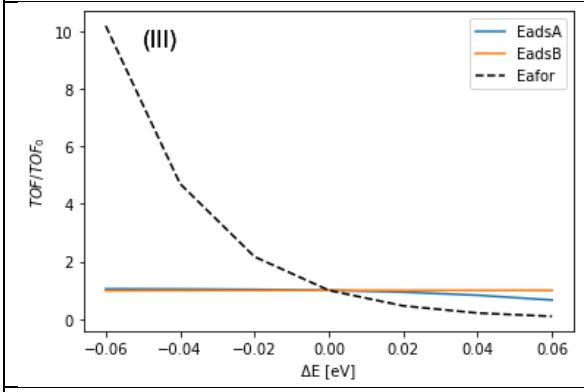

III. Monomolecular reaction

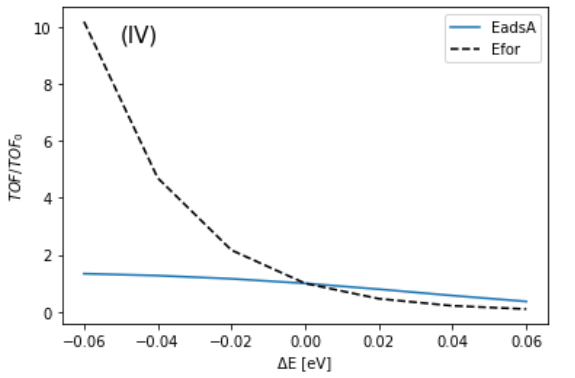

IV. Eley - Rideal reaction with a gaseous product

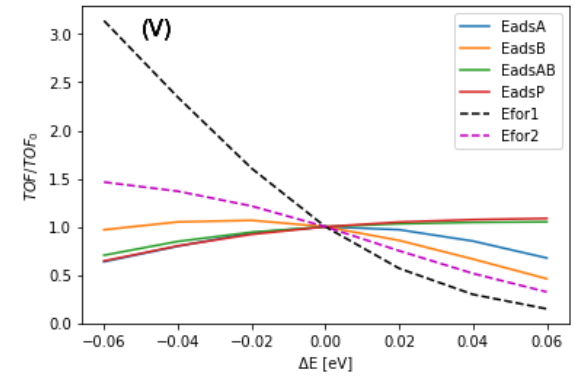

V. Sequential reaction

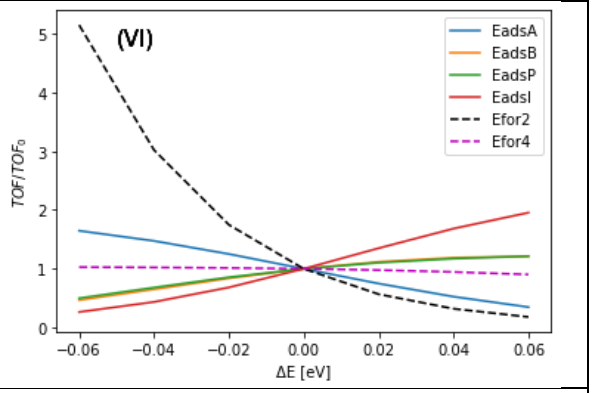

VI. Two-step reaction

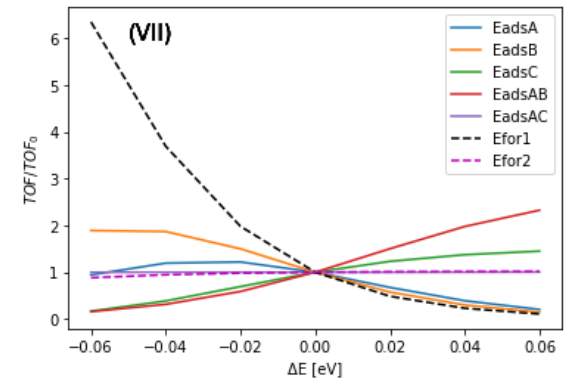

VII. Competitive reaction (AB product)

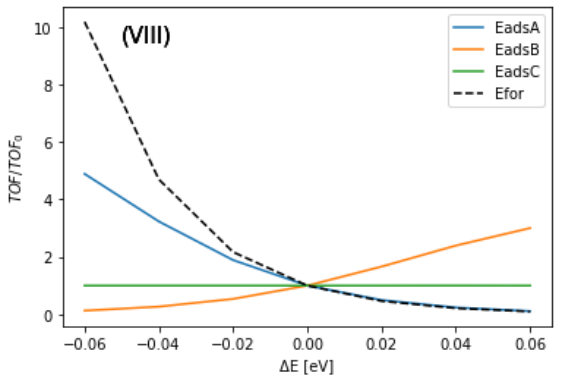

VIII. Dissociation reaction (product B)

Figure 7: A change in the relative turn-over frequency (TOF) when adsorption energies and reaction barriers are changed. Note that in scenarios with more products, the TOFS are plotted for AB product in Competitive reaction mechanism and for B product in Dissociation reaction mechanism. Solid lines present the effect of adsorption energies on TOF while dashed lines represent the effect of forward reaction energies on the TOF effect.

When the surface reaction consists of two sequential steps (Scenarios V and VI), the effect is similar. If the reactants bind more strongly to the surface, the rate can be improved as much as two-fold. However, as seen for reactant B in Scenario V, a too strong interaction begins to impede the reaction, which is in line with the Sabatier principle. On the other hand, decreasing the affinity of the intermediates and the products to the catalyst unequivocally improves the reaction rate.

When two competitive reactions proceed (Scenario VII), the situation is more complex. Binding the reactants more strongly improves the turn-over frequency. However, the magnitude of the effect changes depending if we are changing the adsorption interaction of the more or less strongly bounds reactant. Even a small change of 0.05 eV can accelerate the reaction two-fold. In the dissociation mechanism (Scenario VIII), the trends are clear. A 0.05 eV increase in the reactant adsorption facilitates the reaction 5-fold. The products, however, should bind weakly.

4 Real-world example: ethylene hydrogenation

Lastly, we use a real-world example to showcase the effect of the adsorption energies. We chose the ethylene hydrogenation reaction as it is experimentally feasible and computationally tractable with DFT. We use first-principle data from Qi et al. [19] for the reaction on γ–Al_2O_3 supported carbon-containing Ir_4 clusters. We use the activation barriers and adsorption energies from Qi et al. (see Table 4) and the pre-exponential factor of 10^{-13} s^{-1}. The mechanism is shown in Scheme 3 and is modelled with a system of differential equations (Eq. 31–38).

Scheme 3: The reaction steps in ethylene hydrogenation.

$$\mathrm{H} + * \underset{k_{-H}}{\overset{k_H}{\rightleftharpoons}} \mathrm{H}^*$$

$$\mathrm{C_2H_4} + * \underset{k_{-\mathrm{C_2H_4}}}{\overset{k_{\mathrm{C_2H_4}}}{\rightleftharpoons}} \mathrm{C_2H_4^*}$$

$$\mathrm{C_2H_4^*} + \mathrm{H}^* \underset{k_{-1}}{\overset{k_1}{\rightleftharpoons}} \mathrm{C_2H_5^*} + *$$

$$\mathrm{C_2H_5^*} + \mathrm{H}^* \underset{k_{-2}}{\overset{k_2}{\rightleftharpoons}} \mathrm{C_2H_6^*} + *$$

$$\mathrm{C_2H_6^*} \underset{k_{-\mathrm{C_2H_6}}}{\overset{k_{\mathrm{C_2H_6}}}{\rightleftharpoons}} \mathrm{C_2H_6} + *$$

$$\frac{\partial P_H}{\partial \mathrm{t}} = \left(-\mathrm{k}_H \theta_{empty} P_H + \mathrm{k}_{-H} \theta_H\right) \cdot f \tag{33}$$

$$\frac{\partial P_{C_2H_4}}{\partial t} = \left(-k_{C_2H_4}\theta_{empty}P_{C_2H_4} + k_{-C_2H_4}\theta_{C_2H_4}\right)\cdot f \quad (34)$$

$$\frac{\partial P_{C_2H_6}}{\partial t} = \left(-k_{-C_2H_6}\theta_{empty}P_{C_2H_6} + k_{C_2H_6}\theta_{C_2H_6}\right)\cdot f \quad (35)$$

$$\frac{\partial \theta_H}{\partial t} = k_H\theta_{empty}P_H - k_{-H}\theta_H - k_1\theta_H\theta_{C_2H_4} + k_{-1}\theta_{C_2H_5}\theta_{empty} - k_2\theta_H\theta_{C_2H_4} + k_{-2}\theta_{C_2H_6}\theta_{empty} \quad (36)$$

$$\frac{\partial \theta_{C_2H_4}}{\partial t} = k_{C_2H_4}\theta_{empty}P_{C_2H_4} - k_{-C_2H_4}\theta_{C_2H_4} - k_1\theta_H\theta_{C_2H_4} + k_{-1}\theta_{C_2H_5}\theta_{empty} \quad (37)$$

$$\frac{\partial \theta_C}{\partial t} = k_1\theta_A\theta_B - k_{-1}\theta_C\theta_{empty} - k_2\theta_A\theta_{C_2H_5} + k_{-2}\theta_{C_2H_6}\theta_{empty} \quad (38)$$

$$\frac{\partial \theta_D}{\partial t} = k_2\theta_A\theta_{C_2H_5} - k_{-2}\theta_D\theta_{empty} - k_{C_2H_6}\theta_{C_2H_6} + k_{-C_2H_6}\theta_{empty}P_{C_2H_6} \quad (39)$$

$$\frac{\partial \theta_{empty}}{\partial t} = -k_A\theta_{empty}P_{H_2} + k_{-H}\theta_H - k_{C_2H_4}\theta_{empty}P_{C_2H_4} + k_{-C_2H_4}\theta_{C_2H_4} + k_1\theta_H\theta_{C_2H_4} \quad (40)$$
$$- k_{-1}\theta_{C_2H_5}\theta_{empty} + k_2\theta_H\theta_{C_2H_5} - k_{-2}\theta_{C_2H_6}\theta_{empty} + k_{C_2H_6}\theta_{C_2H_6} - k_{-C_2H_6}P_{C_2H_6}\theta_{empty}$$

We treat all the reactions as reversible and use the same reactor model as described in Section II. We use the same reaction parameters as in Ref [19]. The reaction temperature is 395 K, and the initial hydrogen and ethylene pressure 100 and 50 torr, respectively. There is $3.32 \cdot 10^{-3}$ mol active sites and the catalyst volume is 0.00025 m^3.

Table 4: Energies used in ethylene hydrogenation model

Energy type	Energy value [eV]
$E_{ads}(H_2)$	-2
$E_{ads}(H)$	-1
$E_{ads}(C_2H_4)$	-1.75
$E_{ads}(C_2H_5)$	-3,79
$E_{ads}(C_2H_6)$	-0,27
E_{for1}	1.08
$E_{react.\ 1}^{vacuum}$	-1.57 [20][21] [22]
E_{for2}	0.72
$E_{react.\ 2}^{vacuum}$	-4.36 [20][21][22]

First, we model the reaction with the DFT-calculated values. As shown in Figure 8, the conversion is quantitative after one minute. The catalyst gets quickly saturated with H* (60 %) and ethylene (15 %). As the reaction proceeds, the intermediate (C_2H_5) is observed on the catalyst (5 %), while the coverage of hydrogen is reduced to 0.35. Ethane does not bind noticeably to the surface.

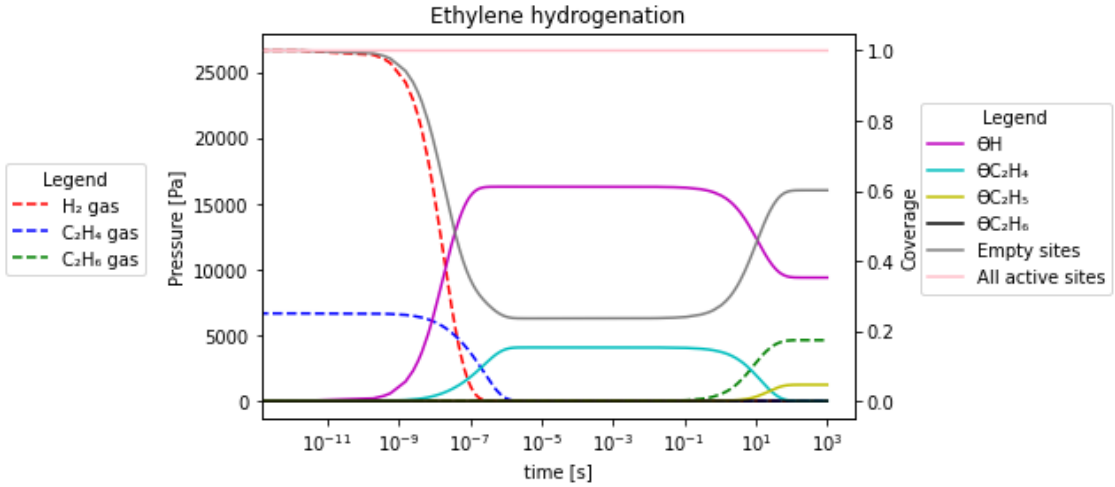

Figure 8: Kinetic modelling of ethylene hydrogenation with kinetic parameters from Ref. 10.1039/c4cp02958e. Dashed lines show the partial pressure of gaseous species, full lines represent catalyst coverages.

Sensitivity analysis show that the reaction is almost exclusively determined by the first hydrogenation reaction (C_2H_4* + H* → C_2H_5* + H*), which has a DRC value of 1.00. The DRC values of other reaction steps, including adsorptions, are negligible (see Table 5).

This can be rationalized as follows. The second reaction step (C_2H_5* + H* → C_2H_6* + *) is faster due to the lower activation barrier and yields a weakly bound product. The rates of adsorptions also do not play an important role because the catalyst is well saturated with reactants or products.

Table 5: DRC values of ethylene hydrogenation steps

Reaction step	DRC value
$E_{ads}(H_2)$	–0,04
$E_{ads}(C_2H_4)$	0.00
$E_{ads}(C_2H_5)$	–0.04
$E_{ads}(C_2H_6)$	0.0
E_{for1}	1.0
$E_{react.1}$	0.0
E_{for2}	0.01
$E_{react.2}$	0.04

However, this *does not* mean that the catalyst cannot be improved by optimising the adsorption interaction of individual species. We vary the adsorption energies of the involved intermediates (H*, C_2H_4*, C_2H_5*, C_2H_6*) and calculated the DRC, which we show in Figure 9. While the adsorption strength of ethane and ethylene does not have a large effect on the DRC values, the adsorption strength of H* and C_2H_5* does. For instance, a moderate change of the adsorption energy of –0.15 eV, which is easily a discrepancy between different flavours of DFT, changes the DRC from 0.00 to +0.75. This calls for extra caution when performing DFT calculations and interpreting their results as even small differences in the calculated energies influence the reaction kinetics.

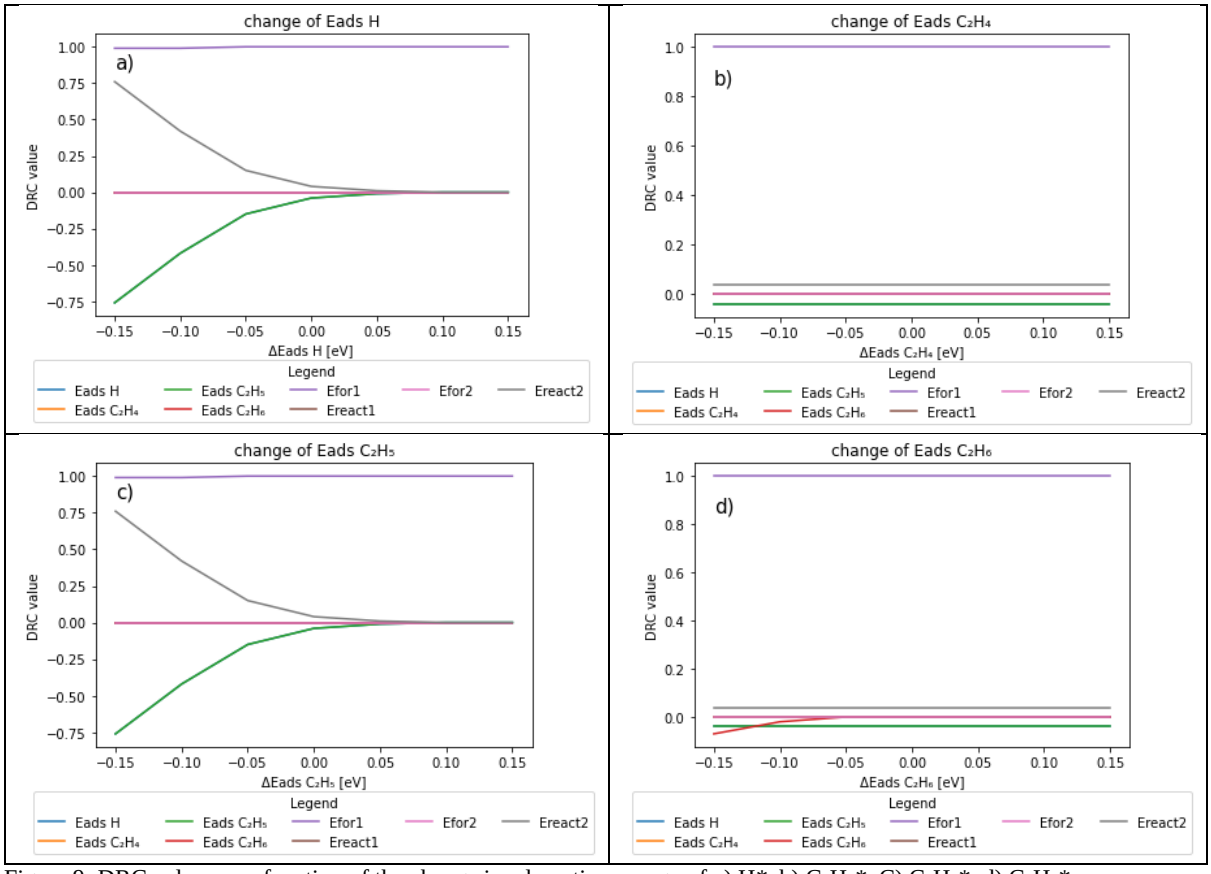

Figure 9: DRC values as a function of the change in adsorption energy of a) H*, b) C_2H_4*, C) C_2H_5*, d) C_2H_6*.

Lastly, we inspect the change in the overall reaction rate when we vary the adsorption rates. While Qi et al. [19] showed that extreme variations of –1 eV in the *co-adsorption* energy increase the reaction rate fourfold, we study the effect of individual adsorption energies. In Figure 10 we show that even by specifically not perturbing the activation barriers, the overall reaction rate is increased when the adsorption energies change.

Changing the adsorption energies of ethylene does not have a major impact on the change of reaction rate, however, lowering the adsorption energies of H_2, C_2H_5* and C_2H_6 decreases the reaction rate, a could be obtained from Figure 10. This is somehow expected since product could not be made if the intermediate is easily desorbed from the catalyst. Lowering the adsorption energy of hydrogen could lead to hydrogen poisoning of the catalysts. Furthermore, ethylene could not adsorb to the catalyst due to high hydrogen coverage.

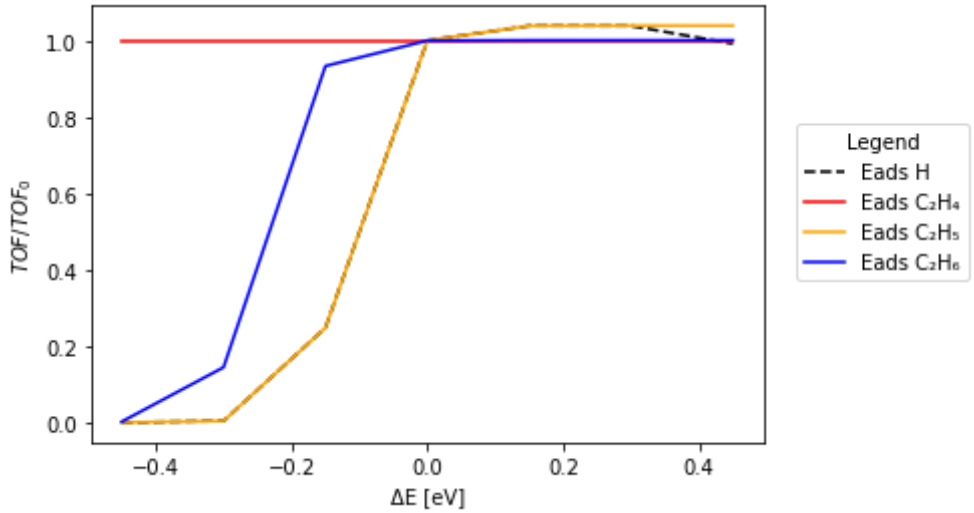

Figure 10: The overall reaction is sensitive to the adsorption energies of the reactants, intermediates and products.

5 CONCLUSION

Modelling various reaction mechanisms of heterogeneous catalysis, we were able to show how adsorption energies effect the reaction rate. We studied the degree of rate control (DRC), which is a generalization of the notion of the rate-determining step (RDS). While the chemical transformation on the surface is generally the RDS, adsorption steps often have non-negligible DRCs. Moreover, even when they are low, small changes in the adsorption energies (<0.2 eV) can increase the DRC for adsorption from <0.10 to 0.7–0.8, making it the RDS.

Furthermore, we studied the overall reaction rate as a function of the adsorption energies. We show that very small changes in adsorption energies (0.06 eV) can increase or decrease the rate of the production formation by up to 50 %. This stands in stark contrast with the common notion of paying attention solely to the activation barriers. Moreover, this underscores the importance of precise calculations of the adsorption energies. The accuracy of density functional theory approaches is usually not on par with the elusive chemical accuracy. The accuracy in the range of 0.1–0.2 eV is commonplace, which can strongly affect the calculated reaction rates, as we have shown.

We demonstrate this on a practical example. Taking real DFT data for ethylene hydrogenation on γ–Al_2O_3 supported carbon-containing Ir_4 clusters, we showed a big influence of the hydrogen adsorption on the ethane production. Interestingly, while the adsorption of ethane and ethylene has a less pronounced effect, the adsorption energy of the intermediate (C_2H_5*) is crucial. Among the chemical transformations, this step (formation of C_2H_5*) predominates.

This research shows that adsorption energies are an important avenue of optimisation when designing better catalysts. Although the activation barriers have the largest cumulative effect on the reaction rate, additional speedup can be attained by fine-tuning the adsorption interaction. This is especially important when the barriers cannot be easily lowered. Usually, reaction barriers and energies are closely intertwined, whereas there is room for improving the adsorption interaction.

Acknowledgements

The authors acknowledge funding from the Slovenian Research Agency (ARRS) through grants J1-3020 (M.H.) and J1-3028 (D.K.), core funding P2-0152 (B.L., L.S.) and infrastructure funding I0-0039.

References

[1] C.M. Friend, B. Xu, Heterogeneous catalysis: A central science for a sustainable future, Acc. Chem. Res. 50 (2017) 517–521. https://doi.org/10.1021/acs.accounts.6b00510.

[2] B. Yang, R. Burch, C. Hardacre, G. Headdock, P. Hu, Understanding the optimal adsorption energies for catalyst screening in heterogeneous catalysis, ACS Catal. 4 (2014) 182–186. https://doi.org/10.1021/cs400727f.

[3] R. Schlögl, Heterogeneous catalysis, Angew. Chemie - Int. Ed. 54 (2015) 3465–3520. https://doi.org/10.1002/anie.201410738.

[4] G.J. Leigh, Haber-Bosch and Other Industrial Processes, Catal. Nitrogen Fixat. (2004) 33–54. https://doi.org/10.1007/978-1-4020-3611-8_2.

[5] J. Teržan, M. Huš, B. Likozar, P. Djinović, Propylene Epoxidation using Molecular Oxygen over Copper-and Silver-Based Catalysts: A Review, ACS Catal. 10 (2020) 13415–13436. https://doi.org/10.1021/acscatal.0c03340.

[6] P. Cossee, Ziegler-Natta catalysis I. Mechanism of polymerization of α-olefins with Ziegler-Natta catalysts, J. Catal. 3 (1964) 80–88. https://doi.org/10.1016/0021-9517(64)90095-8.

[7] C.M. Friend, B. Xu, Heterogeneous catalysis: A central science for a sustainable future, Acc. Chem. Res. 50 (2017) 517–521. https://doi.org/10.1021/acs.accounts.6b00510.

[8] A.J. Medford, A. Vojvodic, J.S. Hummelshøj, J. Voss, F. Abild-Pedersen, F. Studt, T. Bligaard, A. Nilsson, J.K. Nørskov, From the Sabatier principle to a predictive theory of transition-metal heterogeneous catalysis, J. Catal. 328 (2015) 36–42. https://doi.org/10.1016/j.jcat.2014.12.033.

[9] S. Wang, V. Vorotnikov, J.E. Sutton, D.G. Vlachos, Brønsted-evans-polanyi and transition state scaling relations of furan derivatives on pd(111) and their relation to those of small molecules, ACS Catal. 4 (2014) 604–612. https://doi.org/10.1021/cs400942u.

[10] A. Bjelajac, D. Kopač, A. Fecant, E. Tavernier, R. Petrović, B. Likozar, D. Janaćković, Micro-kinetic modelling of photocatalytic CO2 reduction over undoped and N-doped TiO2, Catal. Sci. Technol. 10 (2020) 1688–1698. https://doi.org/10.1039/c9cy02443c.

[11] S. Roy, S. Goedecker, V. Hellmann, Bell-Evans-Polanyi principle for molecular dynamics trajectories and its implications for global optimization, Phys. Rev. E - Stat. Nonlinear, Soft Matter Phys. 77 (2008). https://doi.org/10.1103/PhysRevE.77.056707.

[12] Z. Bin Ding, M. Maestri, Development and Assessment of a Criterion for the Application of Brønsted-Evans-Polanyi Relations for Dissociation Catalytic Reactions at Surfaces, Ind. Eng. Chem. Res. 58 (2019) 9864–9874. https://doi.org/10.1021/acs.iecr.9b01628.

[13] M. Jørgensen, H. Grönbeck, Connection between macroscopic kinetic measurables and the degree of rate control, Catal. Sci. Technol. 7 (2017) 4034–4040. https://doi.org/10.1039/c7cy01246b.

[14] C.T. Campbell, Future Directions and Industrial Perspectives Micro- and macro-kinetics: Their relationship in heterogeneous catalysis, Top. Catal. 1 (1994) 353–366.

https://doi.org/10.1007/BF01492288.
[15] C.T. Campbell, Finding the rate-determining step in a mechanism: Comparing DeDonder relations with the “Degree of Rate Control,” J. Catal. 204 (2001) 520–524. https://doi.org/10.1006/jcat.2001.3396.
[16] C. Stegelmann, A. Andreasen, C.T. Campbell, Degree of rate control: How much the energies of intermediates and transition states control Rates (Journal of the American Chemical Society (2009), 131, (8077-8082)), J. Am. Chem. Soc. 131 (2009) 13563. https://doi.org/10.1021/ja9065199.
[17] C.T. Campbell, The Degree of Rate Control: A Powerful Tool for Catalysis Research, ACS Catal. 7 (2017) 2770–2779. https://doi.org/10.1021/acscatal.7b00115.
[18] C.T. Campbell, The Degree of Rate Control: A Powerful Tool for Catalysis Research, ACS Catal. 7 (2017) 2770–2779. https://doi.org/10.1021/acscatal.7b00115.
[19] K. Qi, J.M. Zhao, G.C. Wang, A density functional theory study of ethylene hydrogenation on MgO- and γ-Al2O3-supported carbon-containing Ir4 clusters, Phys. Chem. Chem. Phys. 17 (2015) 4899–4908. https://doi.org/10.1039/c4cp02958e.
[20] J.A. Manion, Evaluated Enthalpies of Formation of the Stable Closed Shell C1 and C2 Chlorinated Hydrocarbons, J. Phys. Chem. Ref. Data. 31 (2002) 123–172. https://doi.org/10.1063/1.1420703.
[21] W. Tsang, Energetics of Organic Free Radicals, National Institute of Standards and Technology, Martinho Simoes, J.A.; Greenberg, A.; Liebman, J.F., eds., Blackie Academic and Professional, London, 1996.
[22] M.W.. J. Chase, NIST-JANAF Themochemical Tables, Fourth Edition, J. Phys. Chem. Ref. Data, Monogr. 9. (1998) 1–1951.